

Introduction

Recent interest in spherical arrays^{1, 2, 3} for obtaining hemispherical coverage is based on their natural ability to provide more nearly identical high-directivity beams compared with multiplanar arrays.⁴ This paper presents the results of an analytical study of the beam forming properties of a spherical array consisting of thousands of circularly polarized elements on a sphere over 20 wavelengths in diameter. Elements are distributed by means of an icosahedron geometry, resulting in the best possible uniformity of element spacing, which varies less than ± 9 percent from the mean value of 0.73 wavelength. Computed scalar diffraction patterns for various conditions of element excitation are presented in terms of normalized patterns. In particular, the effects of how much of the sphere is active for each beam are presented, along with the effects of element pattern shapes and amplitude distributions. It is shown that an active cap of 140 degrees subtended angle can be used to obtain directive beams with moderately low sidelobes (-20 to -23 dB) over hemispheric coverage regions. Also, spherical arrays allow the use of significantly larger element spacings before grating lobes become objectionable, as compared with spacings required in planar or cylindrical arrays.

Pattern Computations

In computing scalar diffraction patterns, a coordinate system as shown in figure 1 was used, and the array elements were located by means of an icosahedron geometry shown in figure 2. The derived distribution of elements resulted in a near-optimum uniformity of spacing, which varied less than ± 9 percent from a mean value of $S = 0.73$ wavelengths.

Each circularly-polarized element was assumed to have a rotationally-symmetric radiation pattern about its axis, radially oriented as shown in figure 1. For the initial far-field pattern computations described in this paper, the element was assumed to radiate perfect circular polarization throughout its pattern, and mutual coupling effects were not included.

Reference patterns were first computed for assumed isotropic elements with uniform amplitude distribution and ideal phase excitation, as a function of how much of the hemisphere is active. Under these conditions, an entire hemisphere of active elements results in a 3-dB beamwidth factor of $50.5 \lambda/D$ and first sidelobe levels of -13 dB, as shown in figure 3, which also shows a typical pattern for an active cap subtending a half-angle of $\gamma = 50$ degrees. Values of first sidelobe level and beamwidth factor for various active cap angles are shown in figure 4. As the active portion of the hemisphere is reduced toward the limiting case of a nearly planar disc of elements (i.e., $\gamma \rightarrow 0$), the beamwidth factor and sidelobe level approach those of a first-order Bessel function pattern, namely $59 \lambda/D$ and -17.6 dB respectively.

The far-field patterns of major interest are those calculated for more realistic element patterns and amplitude distributions. An active portion of the hemisphere subtending a cone-angle of 140 degrees ($\gamma = 70$ degrees) was found to be near optimum for reasonable element pattern approximations. The effects of cosine amplitude taper is shown typically in figure 5, which applies to isotropic elements, $H(\theta) = 1.0$. When realistic element patterns are used along with amplitude tapering, the resulting radiation pattern is as shown in figure 6. For this typical "realistic" pattern, measured element patterns were approximated by a three-term cosine power series.

Also of interest is the dependence of pattern characteristics on element spacing, which was studied by computing wide-angle far-field patterns for various array diameters, with all other conditions held constant. The results showed that grating lobes do appear as predicted but are greatly suppressed compared with planar arrays. For example, a spherical array with average element spacings of $S \approx \lambda$, a broad grating lobe appears at about 75 degrees from the main beam, but its amplitude is at a -27 dB level.

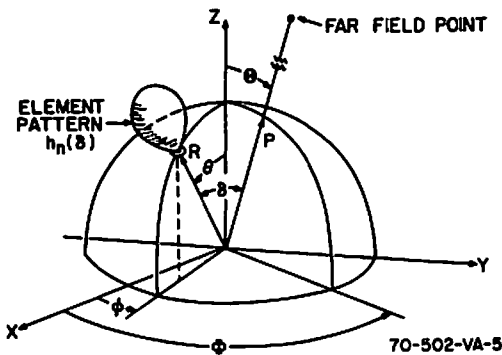


Figure 1. Coordinate System

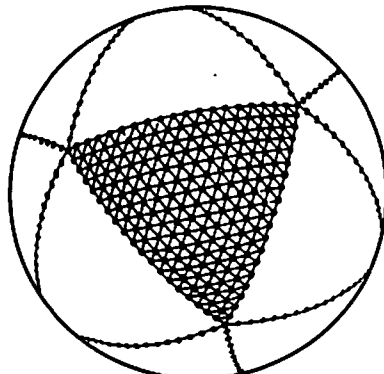


Figure 2. Icosahedron Geometry

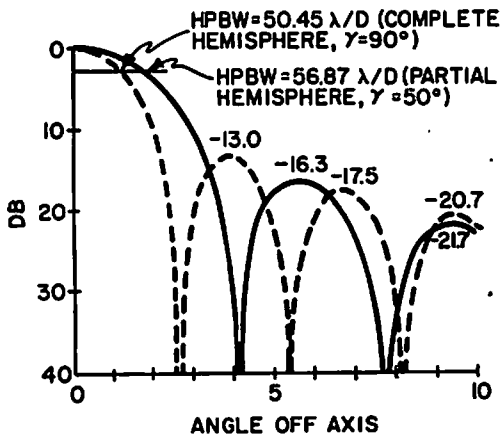


Figure 3. Normalized Spherical Array Patterns

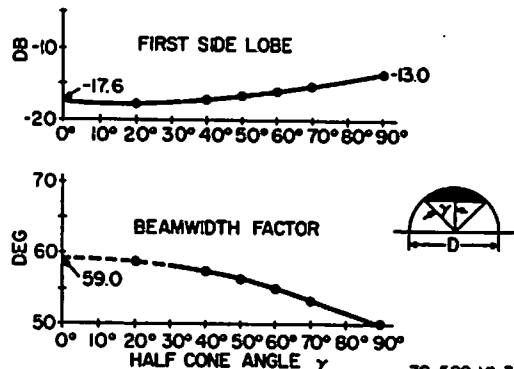


Figure 4. Various Spherical Arrays

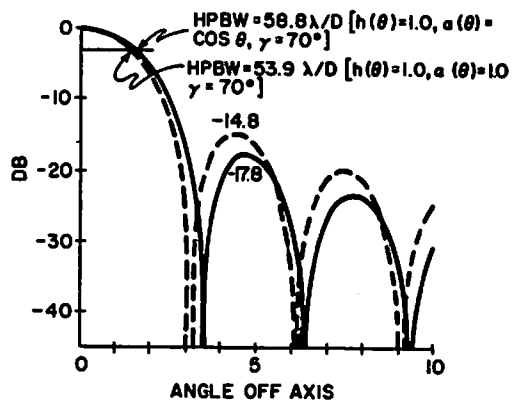


Figure 5. Effect of Cosine Amplitude Taper

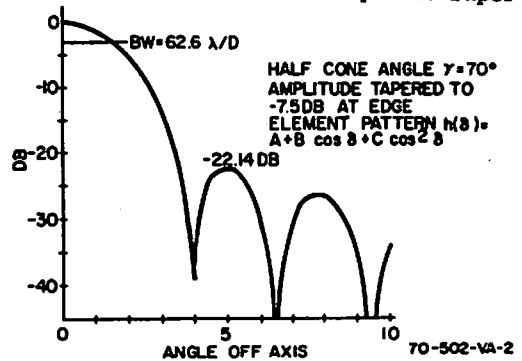


Figure 6. Spherical Array of Circular Waveguide Elements

1. Sengupta, D.L. et al, "Radiation Characteristics of a Spherical Array of Circularly Polarized Elements," *IEEE Trans. Antennas and Prop.*, Vol. AP-16, Jan. 1968, pp. 2-7.
2. Chan, Ishamaru, and Sigelmann, "Equally Spaced Spherical Arrays," *Radio Science*, Vol. 3, No. 5, May 1968, pp. 401-404.
3. Chan, A.K. and R.A. Sigelmann, "Experimental Investigation on Spherical Arrays," *IEEE Trans. Antennas and Prop.*, Vol. AP-17, May 1969, pp. 348-349.
4. Knittel, G.H., "Choosing the Number of Faces of a Phased-Array Antenna for Hemisphere Scan Coverage," *IEEE Trans. Antennas and Prop.*, Vol. AP-13, Nov. 1965, pp. 878-882.